Manganese-induced trafficking and turnover of GPP130 is mediated by sortilin

Swati Venkat and Adam D. Linstedt*
Department of Biological Sciences, Carnegie Mellon University, Pittsburgh, PA 15213

ABSTRACT **Elevated, nontoxic doses of manganese (Mn) protect against Shiga toxin-1–induced cell death via down-regulation of GPP130, a cycling Golgi membrane protein that serves as an endosome-to-Golgi trafficking receptor for the toxin. Mn binds to GPP130 in the Golgi and causes GPP130 to oligomerize/aggregate, and the complexes are diverted to lysosomes. In fact, based on experiments using the self-interacting FM domain, it appears generally true that aggregation of a Golgi protein leads to its lysosomal degradation. How such oligomers are selectively sorted out of the Golgi is unknown. Here we provide evidence that Mn-induced exit of GPP130 from the *trans*-Golgi network (TGN) toward lysosomes is mediated by the sorting receptor sortilin interacting with the lumenal stem domain of GPP130. In contrast, FM-induced lysosomal trafficking of the Golgi protein galactosyltransferase was sortilin independent and occurred even in the absence of its native lumenal domain. Thus sortilin-dependent as well as sortilin-independent sorting mechanisms target aggregated Golgi membrane proteins for lysosomal degradation.**

Monitoring Editor
Keith E. Mostov
University of California, San Francisco

Received: May 26, 2017
Revised: Jul 17, 2017
Accepted: Jul 24, 2017

INTRODUCTION

More than a million deaths occur annually due to Shiga toxin (STx)–producing bacteria, which include *Shigella dysenteriae* and the Shiga toxigenic group of *Escherichia coli* (Beddoe *et al.*, 2010). Shiga toxins invade cells by binding to a cell surface glycolipid followed by endocytosis to early endosomes (Mallard and Johannes, 2003). There, they evade lysosomal degradation by actively sorting into membrane tubules destined for the Golgi complex, a key step in their retrograde trafficking to exert cytotoxicity (Johannes and Wunder, 2011; Mukhopadhyay and Linstedt, 2013). Significantly, for two toxin types, STx and STx1, this sorting is blocked in cells that have had prior exposure to elevated extracellular manganese (Mn). Indeed, nontoxic doses of Mn protect cultured cells and mice from STx1-induced death (Mukhopadhyay and Linstedt, 2012).

Mn sensitivity of STx/STx1 arises because Mn down-regulates GPP130, which serves as a host-cell trafficking receptor for these toxins (Mukhopadhyay and Linstedt, 2012). GPP130 is a *cis*-Golgi localized integral membrane protein that constitutively cycles between early endosomes and the Golgi (Linstedt *et al.*, 1997). A surface loop present in the STx/STx1 pentameric B subunit binds at or near a seven-residue stretch in the coiled-coil lumenal stem domain of GPP130, allowing the toxin to "piggyback" its way to the Golgi (Mukhopadhyay *et al.*, 2013). In the absence of GPP130, the toxins are degraded because instead of gaining access to Golgi-directed membrane tubules, they remain in the central cavity of endosomes, which then mature into multivesicular bodies (MVBs) and lysosomes (Mukhopadhyay and Linstedt, 2012).

GPP130 down-regulation by Mn may relate to homeostatic control of cellular Mn. While Mn is essential, high cytoplasmic levels are toxic (Missiaen *et al.*, 2004; Olanow, 2004; Bouchard *et al.*, 2007). The Mn transporter SPCA1 is Golgi localized and required for GPP130 down-regulation (Mukhopadhyay and Linstedt, 2011). Loss of SPCA1 sensitizes cells to Mn exposure, and a hyperactive mutation of SPCA1 protects against toxic Mn levels (Culotta *et al.*, 2005; Leitch et al., 2011; Mukhopadhyay and Linstedt, 2011). It is thought that active transport of Mn by SPCA1 reduces cytoplasmic Mn concentrations, allowing Mn to be expelled by exocytosis.

The mechanism of Mn-induced GPP130 down-regulation is beginning to emerge. Upon Mn treatment, GPP130 leaves its Golgi-endosome recycling route and instead is diverted from the TGN to

This article was published online ahead of print in MBoC in Press (http://www.molbiolcell.org/cgi/doi/10.1091/mbc.E17-05-0326) on August 2, 2017.

*Address correspondence to: Adam D. Linstedt (linstedt@cmu.edu)

Abbreviations used: AP, FK506 analogue AP21998; FM, $F_{36}M$ substitution of FKBP12; GGA, γ-adaptin homologous ARF-interacting protein; GPP130, Golgi phosphoprotein of 130 kDa; GT, beta 1,4-galactosyltransferase; MVB, multivesicular body; STx, Shiga toxin; TGN, *trans*-Golgi network.

MVBs and then to lysosomes, where it is degraded (Mukhopadhyay *et al.*, 2010). Redistribution is via the canonical TGN-to-lysosome pathway as it requires the clathrin vesicle coat complex and its Golgi-localizing γ-adaptin homologous ARF-interacting protein 1 (GGA1) adaptor (Tewari *et al.*, 2015). The trafficking depends on the late endosome GTPase Rab7 but not its early endosome counterpart Rab5 (Mukhopadhyay *et al.*, 2010). The trigger appears to be Mn-induced clustering of GPP130 dimers into higher-order oligomers. Mn directly binds the GPP130 lumenal stem domain, and the binding causes reversible formation of higher-order oligomers (Tewari *et al.*, 2014). Clustering occurs in the Golgi, and, critically, Mn-induced oligomerization is both required and sufficient for GPP130 redistribution to lysosomes (Tewari *et al.*, 2014).

Rather than being unique to GPP130, oligomerization may be a general trigger of Golgi protein exit and lysosomal degradation, possibly used for Golgi quality control (Tewari *et al.*, 2015). That the region of GPP130 that binds Mn and oligomerizes contains a transferable activity suggests that other Golgi proteins contain the potential for this trafficking behavior if forced to form higher-order oligomers (Tewari *et al.*, 2014). Indeed, the placement of an array of self-interacting FM domains on the lumenal domain of a number of Golgi proteins causes their oligomerization-induced degradation in lysosomes (Tewari *et al.*, 2015). Similar to Mn-induced GPP130 redistribution, FM-induced Golgi protein redistribution is clathrin and GGA1 dependent (Tewari *et al.*, 2015). Also, another Mn-sensitive Golgi protein was recently identified. Although the role of oligomerization was not tested, TMEM165 moves to lysosomes in Mn-treated cells in a manner analogous to that of GPP130 (Potelle *et al.*, 2017). Additionally, the TGN-localized protease furin forms aggregates correlating with its exit from the Golgi and degradation in lysosomes (Wolins *et al.*, 1997).

This apparent generality raises a significant question. If formation of higher-order oligomers is sufficient to alter trafficking of unrelated Golgi proteins, how are they selectively recognized and partitioned into membrane domains coated with GGA1 and clathrin? GPP130 redistribution occurs in the absence of its cytoplasmic domain, suggesting participation of a membrane spanning sorting receptor. Here we tested the role of sortilin because it is a known TGN-to-lysosome sorting receptor with a lumenal domain capable of binding diverse cargo and a cytoplasmic domain that engages GGA1 and clathrin (Lefrancois *et al.*, 2003; Canuel *et al.*, 2008, 2009; Campbell *et al.*, 2016). We provide evidence that sortilin binds GPP130 and is required for its Mn-induced trafficking. Mn-induced redistribution of TMEM165 was also sortilin dependent. Intriguingly, however, sortilin was not required for FM-induced lysosomal targeting, and this occurred even when lumenal sequences were deleted. Thus, there are both sortilin-dependent and sortilin-independent mechanisms to target aggregated Golgi proteins for lysosomal degradation.

RESULTS

Sortilin is required for Mn-induced redistribution of GPP130 to lysosomes

We focused on sortilin because it mediates TGN sorting toward lysosomes for a diverse set of cargo using the clathrin coat complex and the GGA1 adaptor. HeLa cells were transfected with 20 nM sortilin small interfering RNA (siRNA) and assessed for knockdown 48 h posttransfection by immunoblotting (Figure 1A). Sortilin levels dropped to ~20% of those of the controls at 48 h posttransfection. This time point was used for subsequent experiments.

By immunofluorescence microscopy, the steady-state localization of GPP130 and the Golgi marker giantin were unaffected by the knockdown treatment (Figure 1B, untreated). To ensure that sortilin knockdown did not disrupt the Golgi exit of GPP130 along its normal cycling path to endosomes, we treated the cells with monensin, which is a proton ionophore that neutralizes acidic compartments (Tartakoff, 1983). Monensin has no effect on TGN exit of GPP130 but it blocks its retrieval, thereby trapping the protein in early endosomes (Bachert *et al.*, 2001; Puri *et al.*, 2002). In our experiment, a 1-h monensin treatment trapped a fraction of GPP130 in punctae, and this was equally evident for the sortilin knockdown cells (Figure 1B, monensin). As expected, giantin in both control and knockdown cells remained Golgi localized. Thresholded images of the GPP130 channel are also shown to better visualize the punctae. Quantification of the GPP130 appearance in punctae for independent trials confirmed the lack of effect of sortilin knockdown (Figure 1C). Thus TGN exit of GPP130 under the conditions of the monensin treatment was unaffected by sortilin knockdown.

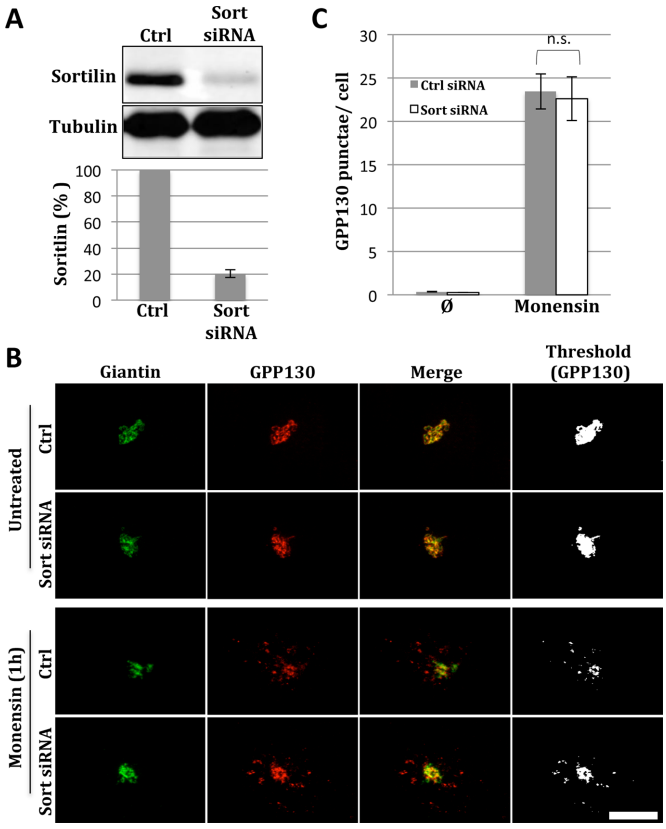

FIGURE 1: Normal GPP130 Golgi localization and redistribution to endosomes in sortilin knockdown cells. (A) To assess knockdown, HeLa cells were untreated or sortilin siRNA-transfected and lysed after 48 h, followed by immunoblotting with anti-sortilin and anti-tubulin antibodies. Quantification shows average values normalized to control cells (±SEM, $n = 3$). (B) Control and sortilin siRNA transfected cells were left untreated (upper rows) or treated with 10 μM monensin for 1 h (lower rows) and stained with anti-giantin (green) or anti-GPP130 (red) antibodies. Merged and thresholded (GPP130 only) images are shown to better visualize the extent of redistribution of GPP130 into endosomal punctae. Bar = 5 μm. (C) Quantified appearance of GPP130 in peripheral punctae of cells that were either control or sortilin siRNA-transfected before or after monensin (Mon) treatment (mean ± SEM, $n = 3$, >15 cells per experiment).

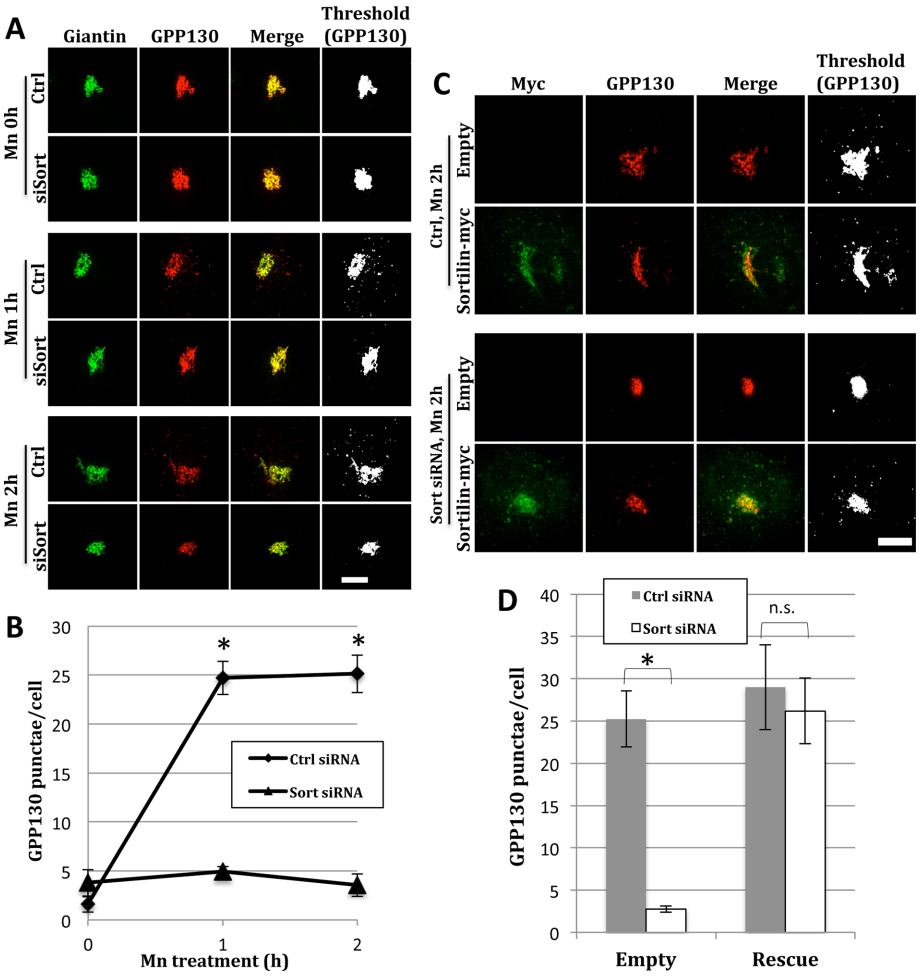

FIGURE 2: Knockdown and rescue of sortilin-dependent, Mn-induced GPP130 redistribution to lysosomes. (A) Control and sortilin knockdown cells were subjected to a 0, 1, or 2 h Mn treatment (500 μM) and fixed and stained using anti-GPP130 (red) and anti-giantin (green) antibodies. Merged and thresholded (GPP130 only) images are also shown for visualization of GPP130 punctae. Bar = 5 μm. (B) Quantification shows the number of GPP130 punctae at each time point of Mn treatment ($n = 3 \pm$ SEM, >15 cells per experiment, $^*p < 0.0006$). (C) To assess rescue, control and sortilin knockdown cells were transfected with a siRNA immune version of the sortilin-myc plasmid or an empty vector. The cells were treated 24 h post–plasmid transfection with 2 h of Mn treatment and then were stained using anti-GPP130 (red) and anti-myc (green) antibodies. Bar = 5 μm. (D) The average number of punctae after the 2 h Mn treatment is quantified for control and knockdown cells (± SEM, $n = 3$, >10 cells per experiment, $^*p < 0.002$).

Rescue with an siRNA immune version of sortilin was used to control against off-target effects. Expression of the myc epitope tagged rescue construct, sortilin-myc, in control cells had no effect on Mn-induced GPP130 redistribution because the redistribution occurred equally in cells transfected with either an empty vector or the same vector containing sortilin-myc (Figure 2C, Ctrl). In contrast, the sortilin-myc construct rescued in that sortilin knockdown blocked redistribution in cells transfected with the empty vector, but the redistribution was restored in cells expressing sortilin-myc (Figure 2C, Sort siRNA). Rescue (≥10 punctae/cell) was observed in 93 ± 7% of cells expressing sortilin-myc (identified by anti-myc staining of the Golgi). Quantification of GPP130 punctae in these independent trials also confirmed the rescue (Figure 2D), showing that the block of the Mn-induced GPP130 redistribution was a specific effect of sortilin absence.

Previous studies have shown that it takes 4–8 h of Mn treatment to cause complete redistribution of GPP130 from the Golgi and its loss of staining due to degradation in lysosomes (Mukhopadhyay *et al.*, 2010). Therefore, we extended the Mn treatment in control and sortilin knockdown cells. As expected, control cells showed a significant loss at 4 h and a nearly complete loss at 8 h (Figure 3A, Ctrl). In contrast, the knockdown cells showed a markedly attenuated response (Figure 3A, Sort siRNA). Quantification revealed that the 25% remaining at 4 h was increased to 75% and that the 5% remaining at 8 h was increased to 45% (Figure 3B). Giantin levels remained stable. That this was a reduction and not a block is typical for membrane trafficking in which cargo gains access to alternate routes or may simply be due to incomplete knockdown. Thus, overall, Mn-induced redistribution and degradation of GPP130 in lysosomes is strongly sortilin dependent. Interestingly, whereas Mn treatment resulted in progressive loss of GPP130 over time, sortilin remained stable (Figure 4, A and B). Thus, if sortilin binds and sorts GPP130 during TGN exit, it is likely that the complex subsequently dissociates so that sortilin can recycle.

Next, control and sortilin knockdown cells were subjected to Mn treatment. As expected, after 1- or 2-h exposures to 500 μM $MnCl_2$, control cells showed a fraction of GPP130 redistributed to punctate structures (Figure 2A, Ctrl) previously identified as prelysosomes or lysosomes based on colocalization with Rab7-GFP (green fluorescent protein) among other measures (Mukhopadhyay *et al.*, 2010; Tewari *et al.*, 2015). Colocalization with Rab7-GFP was also confirmed for the present experiments (Supplemental Figure 1). In striking contrast, sortilin knockdown cells showed little if any GPP130 redistribution (Figure 2A, siSort). Note that giantin staining was unperturbed under these conditions and that the GPP130 channel is again shown after thresholding to better detect faint punctae. Immunoblotting of independent trials confirmed knockdown while quantification of the peripheral punctae clearly supported a strong inhibitory effect of sortilin knockdown (Figure 2B).

Sortilin binds GPP130

To test whether sortilin interacts with GPP130 we used coimmunoprecipitation from cell lysates generated using RIPA lysis buffer, which is nondenaturing but stringent (Seddon *et al.*, 2004). HeLa cells were transfected with GPP130-GFP and the sortilin-myc plasmid. Both transfected constructs were primarily Golgi localized. Immunoprecipitation with anti-myc antibodies yielded a clear recovery of GPP130-GFP from both untreated and Mn treated cells (Figure 5A). In contrast, there was no recovery of GPP130-GFP from cells transfected with the control empty myc vector or in cells not expressing GPP130-GFP. As further evidence of specificity, cotransfection of

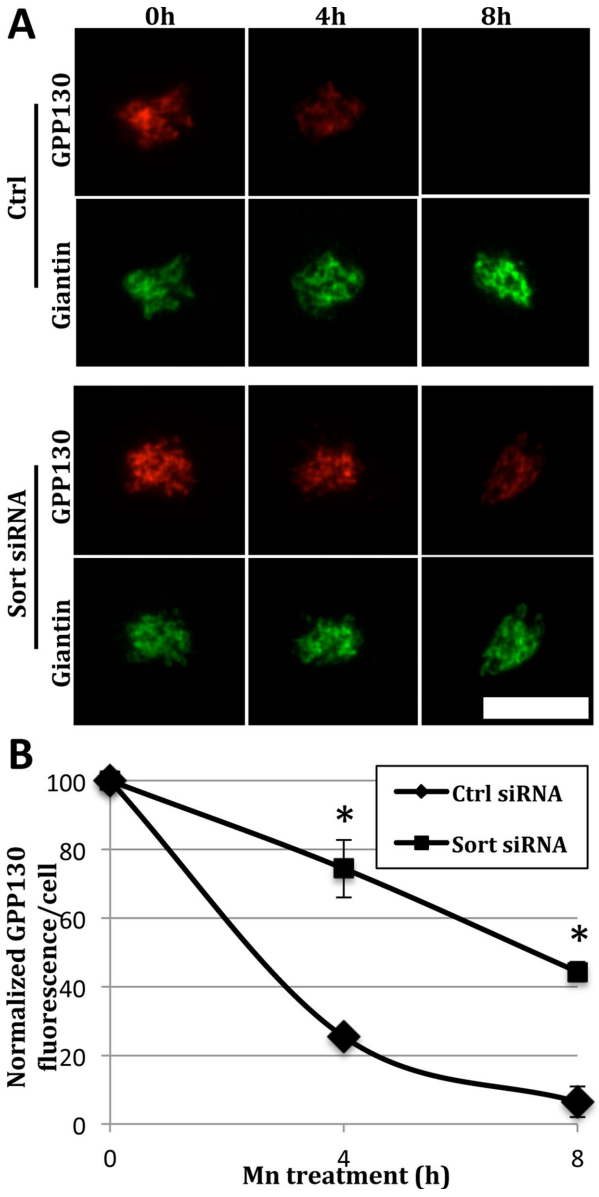

FIGURE 3: Sortilin knockdown attenuates Mn-induced GPP130 degradation. (A) Control and sortilin knockdown cells were subjected to Mn treatment (500 μM) for 0, 4, and 8 h and then stained for GPP130 (red) and giantin (green). Note attenuated decrease of Golgi GPP130 after sortilin knockdown. Bar = 5 μm. (B) Average fluorescence of Golgi localized GPP130 was quantified at each time point of Mn treatment (±SEM, $n = 3$, >15 cells per experiment, $^*p < 0.004$).

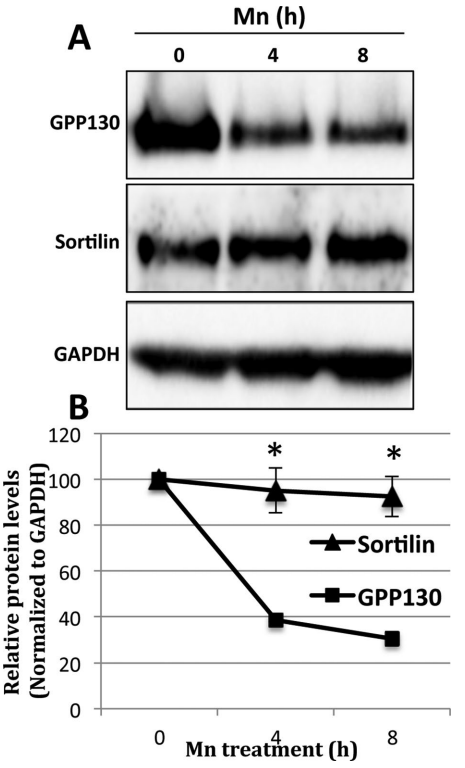

FIGURE 4: Sortilin levels remain stable in Mn treated cells. (A) Cells were subjected to Mn treatment (500 μM) for 0, 4, and 8 h and then immunoblotted to detect sortilin, GPP130, and the loading control GAPDH. (B) Average levels of sortilin and GPP130 were determined after normalization to GAPDH (mean ± SEM, $n = 3$, $^*p < 0.004$).

sortilin with the GPP130-related Golgi protein GP73 (Kladney *et al.*, 2000) yielded little GP73 recovery with sortilin-myc under the identical conditions (Figure 5C, lane 1). There was also little or no interaction detected for endogenous GPP130 presumably because of its low level relative to transfected GPP130-GFP. The interaction is likely direct because, for it to be indirect, the endogenous level of the hypothetical linking component would have to be unexpectedly high relative to endogenous GPP130. It was interesting that sortilin bound GPP130 in untreated cells and that there was no enhancement for Mn-treated cells. This was also the case when 1 mM Mn was added to the lysis buffer in an attempt to preserve oligomerized GPP130 complexes. We interpreted this to mean that GPP130 can form complexes with sortilin even when not oligomerized by Mn, but how Mn enhances sortilin-dependent trafficking remains unclear (see the *Discussion*).

To validate the interaction we attempted the reciprocal coimmunoprecipitation. Lysates from cells that were not Mn treated were subjected to immunoprecipitation using anti-GPP130 antibodies, and anti-myc immunoblotting was used to test for association of sortilin-myc. As shown, there was clear recovery of sortilin-myc only if both GFP-GPP130 and sortilin-myc were present (Figure 5B). Together, the anti-myc and anti-GFP coprecipitation experiments provide strong evidence that the sorting receptor sortilin and its putative cargo GPP130 form reasonably stable complexes when coexpressed, even in the absence of Mn treatment.

Next we attempted to identify a sequence stretch responsible for the interaction. Our focus was on the GPP130 lumenal stem domain because it mediates Mn-induced trafficking of GPP130 (Mukhopadhyay *et al.*, 2010). To investigate whether the lumenal stem domain of GPP130 (residues 36–247) contains a sortilin binding site, we used a previously generated construct in which the lumenal domain is appended to GP73 (Bachert *et al.*, 2007; Mukhopadhyay *et al.*, 2010). GP73 itself does not undergo Mn-induced redistribution to lysosomes, but this behavior is conferred by the addition of the GPP130 stem domain (Mukhopadhyay *et al.*, 2010). Significantly, while GP73 itself yielded only weak recovery, coexpression of GP73-GPP130$_{36\text{-}247}$-GFP with sortilin-myc yielded a strong interaction as indicated by immunoprecipitation with anti-myc antibodies (Figure 5C). To refine the interacting domain, we carried out the same experiment for two additional chimeric

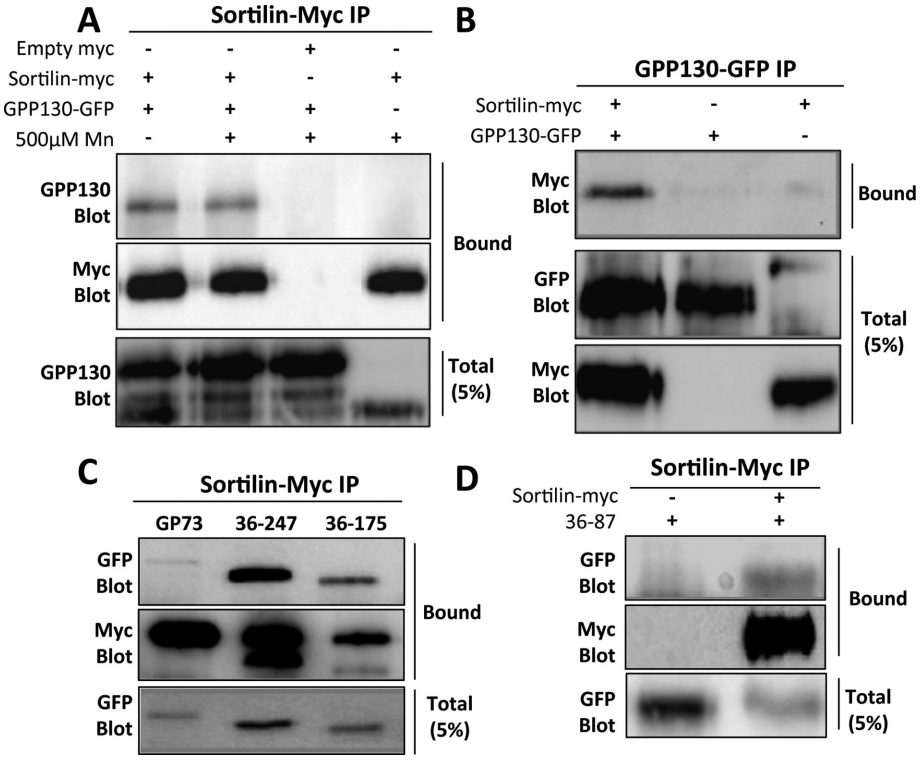

FIGURE 5: GPP130 coprecipitates with sortilin. (A) HeLa cells were transfected with GPP130-GFP, sortilin-myc, or an empty myc plasmid as indicated and then left untreated or Mn-treated (2 h) before lysis and immunoprecipitation using anti-myc antibodies. The immunoblot shown was obtained using anti-GPP130 and anti-myc antibodies and is representative of three trials. Where shown, the 5% total is directly comparable to its corresponding bound fraction, which was analyzed in its entirety. The exposures were identical. (B) The reciprocal experiment was identical except that anti-GPP130 was used for the coimmunoprecipitation ($n = 3$). (C) Cells were transfected with sortilin-myc and GP73, GP73-GPP130$_{36\text{-}247}$, or GP73-GPP130$_{36\text{-}175}$, and immunoprecipitation was carried out using anti-myc followed by immunoblotting with anti-GFP or anti-myc ($n \geq 2$). (D) Cells were transfected with sortilin-myc or GP73-GPP130$_{36\text{-}87}$ as indicated and immunoprecipitation was with anti-myc followed by immunoblotting with anti-GFP or anti-myc ($n = 3$).

constructs, GP73-GPP130$_{36\text{-}175}$-GFP and GP73-GPP130$_{36\text{-}87}$. Each construct was recovered in the presence of sortilin-myc, indicating that the sortilin-binding site in GPP130 likely resides in residues 36–87 (Figure 5, C and D). Interestingly, while GP73-GPP130$_{36\text{-}175}$-GFP retains sensitivity to Mn, GP73-GPP130$_{36\text{-}87}$ is not responsive (Mukhopadhyay *et al.*, 2010) presumably because this construct lacks the residues 88–91 implicated in Mn binding (Tewari *et al.*, 2014). That the sortilin-binding site in GPP130 remains binding competent when separated from the putative Mn-binding site supports the conclusion that sortilin binds GPP130 even in the absence of Mn-induced oligomerization of GPP130.

Mn-induced redistribution of TMEM165 is sortilin dependent

TMEM165 is a conserved, multipass H^+/Ca^{2+} exchanger in the Golgi (Demaegd *et al.*, 2013; Colinet *et al.*, 2016; Potelle *et al.*, 2016). Similar to GPP130, elevated Mn causes TMEM165 to redistribute to lysosomes, where it is degraded (Potelle *et al.*, 2017). Therefore we asked whether TMEM165 redistribution also depends on sortilin. TMEM165 was Golgi localized in untreated cells and then partially redistributed to peripheral punctae after a 2-h Mn exposure (Figure 6A, Ctrl). The kinetics and pattern of the redistribution were similar to those of GPP130. Whereas sortilin knockdown itself had no effect on TMEM165 targeting to the Golgi, it profoundly blocked TMEM165 appearance in punctae after Mn treatment (Figure 6A, siSort). The dependence of TMEM165 redistribution on sortilin was confirmed by quantification of both TMEM165 appearance in punctae (Figure 6B) and TMEM165 loss from the Golgi (Figure 6C).

Sortilin is not required for redistribution of an FM-induced oligomer

Previous work showed that induced oligomerization of several different Golgi resident proteins causes their lysosomal degradation in a manner similar to that of Mn-induced GPP130 degradation (Tewari *et al.*, 2015). These results were obtained by appending an array of three copies of a modified version of the FKBP12 domain, termed an FM domain, to the lumenal domain of the type 2 Golgi membrane proteins (Rizzo *et al.*, 2013). The FM domain self-interacts, but this can be prevented by incubating cells with AP12998 (AP), a modified version of FK506 that is a competitive inhibitor of the interaction (Rivera *et al.*, 2000). Thus AP washout leads to oligomerization and then redistribution from the Golgi to lysosomes. We used an FM-tagged construct based on the Golgi enzyme beta 1,4 galactosyltransferase (GT), to test whether its redistribution depended on sortilin (Tewari *et al.*, 2015). Control and sortilin knockdown cells were transfected with GT-FM-GFP and cultured in the presence of AP. The construct was Golgi localized, and the sortilin knockdown was confirmed by immunoblot. After 24 h, the AP was removed and redistribution of the construct was assayed over time. Redistribution was clearly evident at the 1- and 2-h time points in the control cells and equally evident in the sortilin knockdown cells (Figure 7A). As expected, the Golgi marker giantin remained Golgi localized. Thresholded images of the GT-FM-GFP channel substantiated its presence in peripheral punctae. Quantification of such images for independent trials further validated the lack of effect of sortilin knockdown on redistribution of GT-FM-GFP (Figure 7B). We also tested a version of GPP130 containing FM domains that was previously shown to redistribute upon AP washout (Tewari *et al.*, 2014). In both control and sortilin-knockdown cells, the construct robustly redistributed to punctae after AP washout (Supplemental Figure 2), showing that a GPP130 construct can redistribute independent of sortilin if oligomerized by FM domains. Unfortunately, insolubility of the FM constructs in lysis buffers that preserve the GPP130/sortilin interaction prevented us from testing their ability to bind sortilin. Nevertheless, these findings suggest the presence of a predominant, sortilin-independent mechanism for degradation of Golgi proteins after forced oligomerization by appended FM domains.

Given the sortilin independence and the lack of any obvious sequence similarity among the Golgi proteins that undergo FM-induced degradation (Tewari *et al.*, 2015), we wondered whether the mechanism might be independent of any sequence requirement, at least for

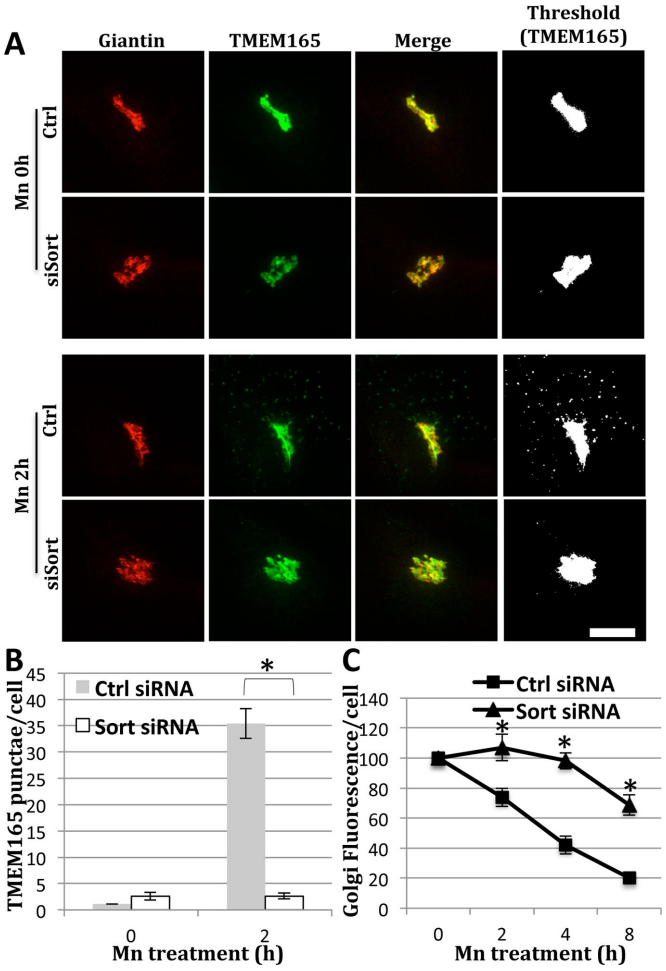

FIGURE 6: TMEM165 redistribution depends on sortilin. (A) Control and sortilin knockdown cells were subjected to a 0 or 2 h Mn treatment (500 μM) and fixed and stained using anti-TMEM165 (green) and anti-giantin (red) antibodies. Merged and thresholded (TMEM165 only) images are also shown. Bar = 5 μm. (B) Quantification shows the average number of TMEM165 punctae at each time point (±SEM, $n = 3$, >15 cells per experiment, $^*p < 0.0003$). (C) Control and sortilin knockdown cells were subjected to Mn treatment (500 μM) for 0, 2, 4, and 8 h and then stained for TMEM165 and giantin. Average fluorescence of Golgi localized TMEM165 was quantified (±SEM, $n = 3$, >15 cells per experiment, $^*p < 0.003$).

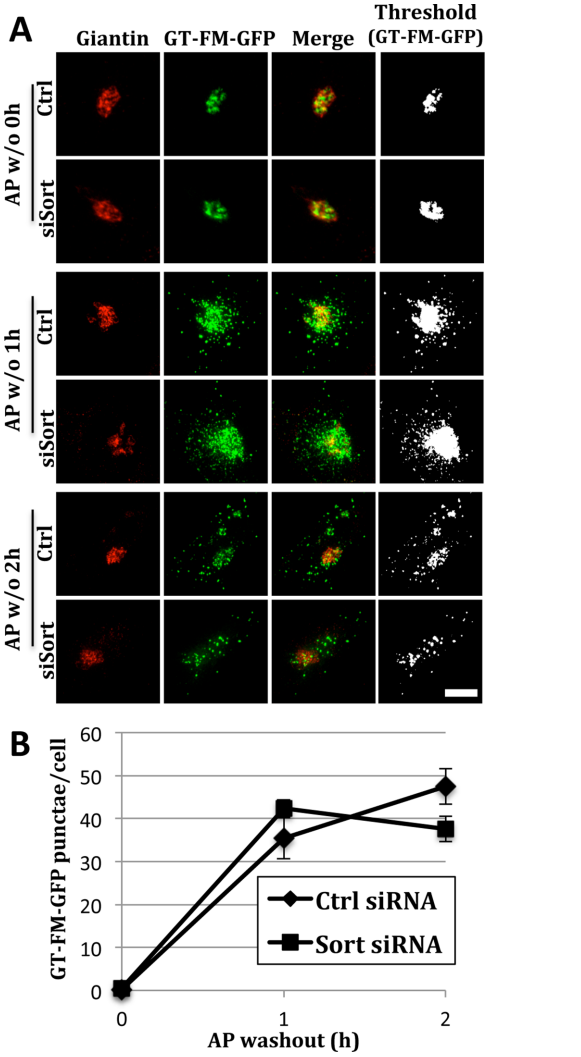

FIGURE 7: FM-induced oligomers redistribute to lysosomes independent of sortilin. (A) Control and sortilin knockdown cells were transfected with GT-FM-GFP and, after 24 h, were subjected to AP washout for 0, 1, or 2 h before staining with anti-giantin antibodies (red) and visualization of GFP fluorescence (green). Merged and thresholded (GFP only) images are also shown. Bar = 5 μm. (B) Quantification shows the number of GT-FM-GFP punctae at each time point (mean ± SEM, $n = 3$, >12 cells per experiment, $p \geq 0.1$).

the lumenal domains of the Golgi proteins. As a test, we removed all remaining GT lumenal sequence from GT-FM-GFP to yield GTΔ_{lum}-FM-GFP. With its cytoplasmic and transmembrane domain left intact to mediate its Golgi targeting, and in the continued presence of AP to prevent its oligomerization, the construct was Golgi localized (Figure 8A, 0 h). However, upon AP washout, it redistributed to lysosomes in a manner indistinguishable from GT-FM-GFP (Figure 8A, 1–2 h). The result was confirmed by quantifying the punctae present for independent trials (Figure 8B). Thus, while Mn-induced GPP130 oligomerization and FM-induced Golgi protein oligomerization are similar in certain respects, the former requires a lumenal sequence stretch and binding to sortilin while the latter requires neither.

DISCUSSION

This study identifies the trafficking receptor sortilin as a key mediator of Mn-induced lysosomal transport and turnover of GPP130. Sortilin knockdown selectively blocked Mn-induced GPP130 trafficking, and this was confirmed by rescue. Sortilin bound GPP130 and the interaction involved a segment of the GPP130 lumenal domain that is required for GPP130 sensitivity to Mn. Because sortilin bound GPP130 even in untreated cells, we speculate that the interaction is normally occurring to mediate turnover of GPP130 and that Mn enhances sorting into this pathway. Interestingly, whereas lysosomal redistribution of TMEM165 was also sortilin dependent, the redistribution FM-induced oligomers of either GPP130 or GT did not depend on sortilin and even occurred without any of the GT lumenal sequence.

At the outset we entertained several ideas for how Mn-induced oligomerization might switch GPP130 sorting away from its normal retrieval and early endosome pathways and into the lysosomal pathway. One was hydrophobic mismatch, referring to a disparity between membrane thickness and transmembrane domain length

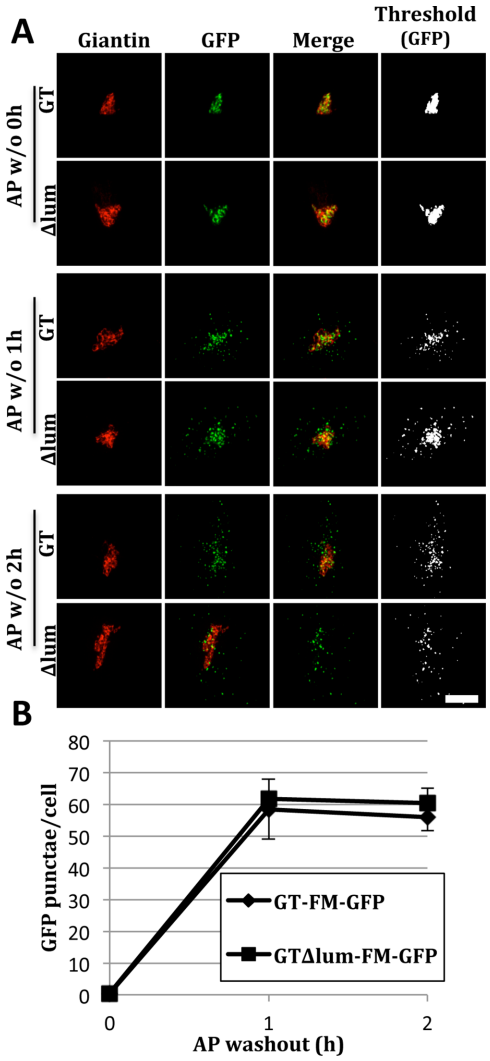

FIGURE 8: Lysosomal redistribution of $GT_{\Delta lum}$-FM-GFP. (A) Cells were transfected with either GT-FM-GFP or $GT_{\Delta lum}$-FM-GFP (all GT lumenal sequence removed) and subjected to an AP washout for 0, 1, or 2 h before staining for giantin and visualization of GFP. Merged and thresholded (GFP only) images are also shown. (B) Quantification shows the number of GFP punctae for the constructs at each time point (mean ± SEM, $n = 3$, >12 cells per experiment, $p \geq 0.3$).

(Destainville *et al.*, 2016). Tilting of a long transmembrane is a strategy to maximize hydrophobic contact in a thinner membrane, but this strategy may fail for a higher-order oligomer because it requires significant displacement of the transmembrane domains relative to one another. Thus, to minimize hydrophobic mismatch of its transmembrane domain, GPP130 might segregate into thicker membrane domains upon oligomerization. The GPP130 transmembrane domain comprises 22 residues, which is relatively long for a Golgi protein. Another idea was avidity, in which the overall affinity of an interaction is increased due to multiple parallel contacts. To achieve avidity-based sorting, a GPP130 oligomer could conceivably engage multiple sites on a putative multivalent receptor. The involvement of sortilin favors the avidity model, especially because sortilin has a 10-bladed beta-propeller lumenal domain suggestive of multivalency (Quistgaard *et al.*, 2009). However, this model predicts increased recovery of GPP130 with sortilin in Mn-treated cells, which was not observed (Figure 5A).

Currently, we favor the idea that the switch from normal cycling to degradation is the result of accelerated access to a normal, sortilin-mediated, turnover pathway. This might be attributed to two effects of oligomerization: steric exclusion from the other pathways and greater efficiency of the sortilin pathway due to the increased GPP130 in each sorting complex. Exclusion of large proteins or protein complexes from small vesicles, such as Golgi retrieval vesicles, has been observed (Rivera *et al.*, 2000; Rizzo *et al.*, 2013). In a similar manner, oligomerized GPP130 may be excluded from the Golgi retrieval and endosomal recycling pathways. Clearly, it is not excluded from the lysosomal pathway, implying that this clathrin/GGA1-mediated pathway has the flexibility to accommodate large complexes. Anterograde transport of large cargo, including collagen, is well documented and takes place using alternative mechanisms and/or unexpected geometric flexibility in vesicle coat complexes (Malhotra and Erlmann, 2015; Saito and Katada, 2015; Gorur *et al.*, 2017). At the same time, if access of GPP130 to the canonical lysosomal pathway is governed by binding to sortilin and sortilin is limiting (as might well be expected), then oligomers will be more efficiently sorted than dimers. That is, each sortilin-GPP130 interaction would capture many more GPP130 molecules when GPP130 is oligomerized. The size range of the GPP130 oligomers is not known, so the stoichiometry cannot be estimated. Also, these stoichiometrically unbalanced sortilin-GPP130 complexes likely disassemble upon cell lysis, leaving each sortilin bound only to the GPP130 dimer it directly contacted because the Mn-dependent contacts between GPP130 dimers are rapidly reversible upon chelation or dilution of Mn (Tewari *et al.*, 2014). This would explain the equal recovery of GPP130 by sortilin immunoprecipitation from untreated and Mn-treated cells (Figure 5A), although it is confounding that such dissociation, if present, was not counteracted by supplementing the lysis buffer with Mn. In any case, the binding of GPP130 to sortilin in untreated cells can be explained as mediating normal turnover of GPP130, which exhibits a half-life of roughly 18 h (Linstedt *et al.*, 1997). While constitutive, it would normally account for only a small fraction of GPP130 due to competition from the retrieval and recycling pathways. Then, upon oligomerization by Golgi Mn, the GPP130 clusters would bind sortilin with higher stoichiometry while simultaneously failing to enter the other routes because of steric exclusion.

Because FM-induced oligomers are sortilin independent and require neither cytosolic (Tewari *et al.*, 2015) nor lumenal sequence, their sorting mechanism might be quite novel. If it requires some shared aspect of the transmembrane domains, it could be receptor-mediated or perhaps involve hydrophobic mismatch. While hydrophobic mismatch could explain segregation of the oligomerized clusters in the membrane, it would still require an explanation for how clathrin and GGA1 recognize this patch. Candidate receptors might include sortilin-related receptor proteins SorLA and SorCS or either of the mannose-6-phosphate receptors, but each of these is known for binding lumenal cargo not transmembrane domains (Ghosh *et al.*, 2003; Willnow *et al.*, 2008; Braulke and Bonifacino, 2009; Hermey, 2009). Also, hydrophobic mismatch should depend on transmembrane domain length, and shortening the transmembrane domain of an FM-containing construct by deleting five residues did not prevent lysosomal redistribution (our unpublished observations). It is notable that while Mn-induced GPP130 degradation occurs over a period of ~8 h, rapid and almost complete loss of FM-induced oligomers from the Golgi is achieved in ~4 h (Mukhopadhyay *et al.*, 2010; Tewari *et al.*, 2015). We expect the FM-induced oligomeric units to be more stable and perhaps much larger than Mn-induced GPP130

oligomers. They may also impart strong effects on membrane curvature because FM domains interact in an anti-parallel orientation that can zipper together opposed membranes (Rivera *et al.*, 2000; Rizzo *et al.*, 2013). Perhaps their sorting is simply the consequence of strong exclusion from any other pathway except toward lysosomes. This possibility highlights the significance of understanding the mechanism of size flexibility in the clathrin/GGA1 pathway.

In conclusion, this work shows that sortilin binds to the coiled-coil lumenal domain of GPP130 and mediates its lysosomal trafficking and turnover under elevated Mn conditions. Lysosomal targeting of FM-induced oligomers is sortilin independent and indicates that there exists an alternate, possibly sequence-independent, quality control pathway operating at the Golgi that mediates their clearance. Future studies will aim to test for direct interaction between sortilin and GPP130 and map GPP130 residues required for this binding in order to elucidate the underlying interaction mechanism.

MATERIALS AND METHODS

Antibodies and general reagents

Monoclonal antibodies were against GPP130 (Linstedt *et al.*, 1997), myc (Evan *et al.*, 1985; Jesch *et al.*, 2001), HA (H3663, Clone HA-7; Sigma), giantin (Linstedt and Hauri, 1993), GFP (SAB2702197, clone GT859; Sigma), sortilin (Cat# 612100, clone 48/Neurotensin; BD Biosciences), and tubulin (T6557, clone GTU-88; Sigma). Polyclonal antibodies were against GPP130 (Puri *et al.*, 2002), TMEM165 (NBP1-90651; Novus Biologicals), GAPDH (14C10; Cell Signaling Technology), and sortilin (a kind gift from Claus M. Petersen, Aarhus University [Petersen *et al.*, 1997]). Secondary antibodies were Alexa 488 anti-mouse (Cat#A28175; Thermo Fisher Scientific), Alexa 488 anti-rabbit (Cat#A27034; Thermo Fisher Scientific), Alexa 555 anti-rabbit (Cat#A27039; Thermo Fisher Scientific), Alexa 555 anti-mouse (Cat#A28180; Thermo Fisher Scientific), and horseradish peroxidase–conjugated goat anti-mouse (Cat#170-6516; Sigma) and goat anti-rabbit antibodies (Cat#170-6515; Sigma). AP12998 was from Clontech (called D/D solubilizer, Cat#635054). Cycloheximide (Cat#C7698) and monensin (Cat#M5273) were from Sigma. ECL blotting substrate (Cat#32209) and $MnCl_2$ (Cat#M87-500) were from Thermo Fisher Scientific.

Constructs and transfection reagents

Primers were purchased from Integrated DNA Technologies. The sortilin-myc construct was a kind gift from Stephane Lefrancois, McGill University (Lefrancois *et al.*, 2003). Silent mutations to confer siRNA resistance were introduced using the Phusion DNA polymerase (F530S; Thermo Fisher Scientific) as per the manufacturer's protocols (forward primer 5′-CCTCCGTGGGACAGGAACA**A**TT-**T**TA**C**TCTATTCTGGCAGCAAAT-3′ with mutations highlighted). The construct was verified by sequencing. GT-FM-GFP and GPP130-FM-GFP were previously described (Rizzo *et al.*, 2013; Tewari *et al.*, 2015). To create $GT_{\Delta lum}$-FM-GFP, the remaining 20-amino-acid lumenal domain of GT from the GT-FM-GFP plasmid was looped out (forward primer 5′-GGATCCGAGCTCGGTGAAGC-3′) using Pfu Turbo DNA polymerase (Cat#600250; Agilent Technologies). The construct was verified by sequencing. The constructs Rab7-GFP, GP73-$GPP130_{36\text{-}247}$, GP73-$GPP130_{36\text{-}87}$, and GP73-$GPP130_{36\text{-}175}$ were previously described (Mukhopadhyay *et al.*, 2010). Control siRNA (5′-GACCAGCCAUCGUAGUACUtt-3′) and sortilin siRNA (SORT1HSS109429, Catalog#: 1299001) were purchased from Thermo Fisher Scientific. DNA and siRNA transfections were carried out using JetPEI (Cat#101-40N; Polyplus-transfection) and JetPRIME (Cat#114-07; Polyplus-transfection), respectively, as per the manufacturer's protocols.

Cell culture and experimental treatments

HeLa cells (Cat# ATCC-CCL-2, CVCL_0030) were grown in MEM (Cat#10-010-CV; Corning) containing 10% fetal bovine serum (FBS; Cat#S111150; Atlanta Biologicals) at 37°C, 5% CO_2. All cell lines were verified mycoplasma free every 2 mo using Hoechst staining. For immunofluorescence experiments, cells were plated on 12-mm coverslips in 35-mm or 24-well plates, and after 16 h, each plate (~50% confluent) was transfected with control or sortilin siRNA at a final concentration of 20 nM. After 48 h, the medium was replaced with fresh medium alone or with 500 μM $MnCl_2$ or 10 μM monensin for the indicated times. The coverslips were then collected and analyzed by immunofluorescence while the cells remaining behind in the 35-mm plates were analyzed by immunoblot to determine knockdown efficiency. For rescue experiments, the cells were siRNA-transfected (20 nM) at 80% confluence and then grown 24 h before being transfected with plasmid. Fresh medium was substituted after 8 h and then, after 24 h, 500 μM $MnCl_2$ was added for the indicated times. Analysis was restricted to cells with moderate expression. Controlled polymerization experiments were essentially as described (Tewari *et al.*, 2015). Cells at 80% confluence were siRNA-transfected (20 nM), and then after 24 h they were plasmid-transfected and allowed to recover another 8 h. They were then cultured 16 h in fresh medium containing 1 μM AP with the last 30 min containing both AP and cycloheximide. At this point the AP washout began for the indicated times and in the continued presence of cycloheximide. To determine sortilin stability, HeLa cells grown in 35-mm plates to 80% confluency were treated as indicated then washed twice with phosphate-buffered saline (PBS) and lysed in reducing sample buffer (156 mM Tris, pH 6.8, 10% SDS, 50% glycerol, 5% β-mercaptoethanol, 0.1% bromophenol blue, 6 M urea) before immunoblotting. For other immunoblotting experiments, cells at 50% confluence were siRNA-transfected (20 nM) and allowed to recover for 2 d before treatment with 500 μM $MnCl_2$ for the indicated times. For immunoprecipitation, HeLa cells were grown in 10-cm plates to ~70% confluency and transfected with the indicated pairs of plasmids. Fresh medium was substituted after 8 h and then, after 16 h, the medium was left alone or adjusted to 500 μM $MnCl_2$ for the final 2 h of incubation.

Immunofluorescence

Generally, cells were fixed with 3% paraformaldehyde for 15 min, washed 5x with PBS (137 mM NaCl, 2.7 mM KCl, 6.5 mM Na_2HPO_4, 1.5 mM KH_2PO_4), permeabilized for 30 min with block solution (PBS containing 0.1% Triton X-100, 5% FBS, and 0.2 M glycine), and then incubated in ~150 μl primary antibody solution (diluted in block) on a shaker at room temperature (RT) for 1 h. GPP130 and/or giantin were detected using a polyclonal anti-GPP130 and monoclonal anti-giantin, respectively, at 1:1000 dilution. After five washes with PBS, the coverslips were incubated with secondary antibodies at a 1:1000 dilution in block solution for 30 min at RT on a shaker. Following five final washes with PBS, the coverslips were attached to glass slides using Gelvatol mounting medium (10.5% polyvinyl alcohol and 21% glycerol in 100 mM Tris, pH 8.5) and observed under a spinning disk confocal microscope as previously described (Tewari *et al.*, 2014). Staining for TMEM165 was exactly the same except that fixation was with 0.5 ml methanol at –20°C for 20 min and the antibody was used at a 1:500 dilution. Images were analyzed using ImageJ (Version 1.50i, http://imagej.nih.gov/ij). To measure mean Golgi fluorescence, background subtraction

was carried out on average value projections generated from individual z-sections of each image. Mean GPP130 or TMEM165 fluorescence in the Golgi was measured via the measure plug-in of ImageJ, using giantin as a mask. Analysis of cytoplasmic punctae was performed as previously described (Tewari *et al.*, 2014). Briefly, maximum value projections were generated from individual z-stacks of an image. These projections were background subtracted and uniformly thresholded to visualize punctae (Mukhopadhyay *et al.*, 2010).

Immunoprecipitation

Cells (10 cm plate) were washed 2X with PBS and then lysed with 0.5 ml RIPA buffer (25 mM Tris, pH 6.8, 150 mM NaCl, 1% NP-40, 0.5% sodium deoxycholate, 0.1% SDS, 1 mM phenylmethylsulfonyl fluoride) and ~15 passes through a 25-gauge needle followed by centrifugation at 14,000 × *g* to remove insoluble material. Aliquots (5% input) of the supernatants were set aside, and the remainders were precleared by rotation with 10 µl Protein G beads (17-0618-01; GE Healthcare) at 4°C for 30 min followed by brief centrifugation for 1 min at 14,000 × *g*. The precleared lysates were then incubated for 1 h at 4°C with antibody (3 µl anti-myc monoclonal or 5 µl anti-GPP130 monoclonal) followed by a 1 h rotation with 10 µl of Protein G beads (50% slurry). The beads were washed 3 × 2 min in 1 ml RIPA buffer at 4°C with rotation. The washed bead and input fractions were then boiled 10 min in reducing sample buffer before immunoblotting.

Immunoblotting

Samples were run alongside a molecular weight ladder (Cat#26619; Thermo Fisher Scientific) on 7% SDS–PAGE gels and then transferred to nitrocellulose membranes (Cat#10600002; GE Healthcare) at 0.3 A for 2 h. The membrane was blocked with 5% nonfat dry milk powder in PBST (PBS + 0.1% Tween-20) for 15 min and then incubated in the same buffer containing the primary antibody 1–18 h on a shaker. Polyclonal anti-GPP130 (1:1000), monoclonal anti-myc (1:500), and monoclonal anti-GFP (1:2000) were used to detect GPP130, sortilin-myc, and GFP tagged GP73-GPP130 chimeric constructs, respectively. Also used were monoclonal (1:500), polyclonal anti-sortilin (1:2000), polyclonal anti-GAPDH, and monoclonal anti-tubulin (1:3000) antibodies. The membrane was washed 10 × 6 min in PBS-T, followed by incubation with HRP-conjugated secondary antibody (1:2000) for 1 h and then another 10 × 6 min washes. The blots were soaked with the ECL substrate and imaged using Chemi-Doc Touch Imaging System followed by analysis with Image Lab software (Version 5.2.1; Bio-Rad).

Statistical analyses

All findings presented were replicated in three or more independent experiments. Comparisons between two groups were performed using a two-tailed Student's *t* test assuming equal variances. In general, $p < 0.05$ was considered significant, and the determined *p* values are provided in the figure legends. Asterisks in graphs, wherever present, denote statistically significant differences.

ACKNOWLEDGMENTS

We thank Collin Bachert, Emily Simon, and Tina Lee for critical advice on the manuscript and Claus Petersen and Stephane Lefrancois for generous reagent gifts. Funding was by National Institutes of Health R01 Grant GM08411101 (to A.D.L.).

REFERENCES

Bachert C, Fimmel C, Linstedt AD (2007). Endosomal trafficking and proprotein convertase cleavage of cis golgi protein GP73 produces marker for hepatocellular carcinoma. Traffic 8, 1415–1423.

Bachert C, Lee TH, Linstedt AD (2001). Lumenal endosomal and Golgi-retrieval determinants involved in pH-sensitive targeting of an early Golgi protein. Mol Biol Cell 12, 3152–3160.

Beddoe T, Paton AW, Le Nours J, Rossjohn J, Paton JC (2010). Structure, biological functions and applications of the AB5 toxins. Trends Biochem Sci 35, 411–418.

Bouchard M, Laforest F, Vandelac L, Bellinger D, Mergler D (2007). Hair manganese and hyperactive behaviors: pilot study of school-age children exposed through tap water. Environ Health Perspect 115, 122–127.

Braulke T, Bonifacino JS (2009). Sorting of lysosomal proteins. Biochim Biophys Acta 1793, 605–614.

Campbell C, Beug S, Nickerson PE, Peng J, Mazerolle C, Bassett EA, Ringuette R, Jama FA, Morales C, Christ A, Wallace VA (2016). Sortilin regulates sorting and secretion of Sonic hedgehog. J Cell Sci 129, 3832–3844.

Canuel M, Korkidakis A, Konnyu K, Morales CR (2008). Sortilin mediates the lysosomal targeting of cathepsins D and H. Biochem Biophys Res Commun 373, 292–297.

Canuel M, Libin Y, Morales CR (2009). The interactomics of sortilin: an ancient lysosomal receptor evolving new functions. Histol Histopathol 24, 481–492.

Colinet AS, Sengottaiyan P, Deschamps A, Colsoul ML, Thines L, Demaegd D, Duchene MC, Foulquier F, Hols P, Morsomme P (2016). Yeast Gdt1 is a Golgi-localized calcium transporter required for stress-induced calcium signaling and protein glycosylation. Sci Rep 6, 24282.

Culotta VC, Yang M, Hall MD (2005). Manganese transport and trafficking: lessons learned from Saccharomyces cerevisiae. Eukaryot Cell 4, 1159–1165.

Demaegd D, Foulquier F, Colinet AS, Gremillon L, Legrand D, Mariot P, Peiter E, Van Schaftingen E, Matthijs G, Morsomme P (2013). Newly characterized Golgi-localized family of proteins is involved in calcium and pH homeostasis in yeast and human cells. Proc Natl Acad Sci USA 110, 6859–6864.

Destainville N, Schmidt TH, Lang T (2016). Where biology meets physics–a converging view on membrane microdomain dynamics. Curr Top Membr 77, 27–65.

Evan GI, Lewis GK, Ramsay G, Bishop JM (1985). Isolation of monoclonal antibodies specific for human c-myc proto-oncogene product. Mol Cell Biol 5, 3610–3616.

Ghosh P, Dahms NM, Kornfeld S (2003). Mannose 6-phosphate receptors: new twists in the tale. Nat Rev Mol Cell Biol 4, 202–212.

Gorur A, Yuan L, Kenny SJ, Baba S, Xu K, Schekman R (2017). COPII-coated membranes function as transport carriers of intracellular procollagen I. J Cell Biol.

Hermey G (2009). The Vps10p-domain receptor family. Cell Mol Life Sci 66, 2677–2689.

Jesch SA, Lewis TS, Ahn NG, Linstedt AD (2001). Mitotic phosphorylation of Golgi reassembly stacking protein 55 by mitogen-activated protein kinase ERK2. Mol Biol Cell 12, 1811–1817.

Johannes L, Wunder C (2011). Retrograde transport: two (or more) roads diverged in an endosomal tree? Traffic 12, 956–962.

Kladney RD, Bulla GA, Guo L, Mason AL, Tollefson AE, Simon DJ, Koutoubi Z, Fimmel CJ (2000). GP73, a novel Golgi-localized protein upregulated by viral infection. Gene 249, 53–65.

Lefrancois S, Zeng J, Hassan AJ, Canuel M, Morales CR (2003). The lysosomal trafficking of sphingolipid activator proteins (SAPs) is mediated by sortilin. EMBO J 22, 6430–6437.

Leitch S, Feng M, Muend S, Braiterman LT, Hubbard AL, Rao R (2011). Vesicular distribution of secretory pathway Ca(2+)-ATPase isoform 1 and a role in manganese detoxification in liver-derived polarized cells. Biometals 24, 159–170.

Linstedt AD, Hauri HP (1993). Giantin, a novel conserved Golgi membrane protein containing a cytoplasmic domain of at least 350 kDa. Mol Biol Cell 4, 679–693.

Linstedt AD, Mehta A, Suhan J, Reggio H, Hauri HP (1997). Sequence and overexpression of GPP130/GIMPc: evidence for saturable pH-sensitive targeting of a type II early Golgi membrane protein. Mol Biol Cell 8, 1073–1087.

Malhotra V, Erlmann P (2015). The pathway of collagen secretion. Annu Rev Cell Dev Biol 31, 109–124.

Mallard F, Johannes L (2003). Shiga toxin B-subunit as a tool to study retrograde transport. Methods Mol Med 73, 209–220.
Missiaen L, Raeymaekers L, Dode L, Vanoevelen J, Van Baelen K Parys JB, Callewaert G, De Smedt H, Segaert S, Wuytack F (2004). SPCA1 pumps and Hailey-Hailey disease. Biochem Biophys Res Commun 322, 1204–1213.
Mukhopadhyay S, Bachert C, Smith DR, Linstedt AD (2010). Manganese-induced trafficking and turnover of the cis-Golgi glycoprotein GPP130. Mol Biol Cell 21, 1282–1292.
Mukhopadhyay S, Linstedt AD (2011). Identification of a gain-of-function mutation in a Golgi P-type ATPase that enhances Mn2+ efflux and protects against toxicity. Proc Natl Acad Sci USA 108, 858–863.
Mukhopadhyay S, Linstedt AD (2012). Manganese blocks intracellular trafficking of Shiga toxin and protects against Shiga toxicosis. Science 335, 332–335.
Mukhopadhyay S, Linstedt AD (2013). Retrograde trafficking of AB(5) toxins: mechanisms to therapeutics. J Mol Med (Berl) 91, 1131–1141.
Mukhopadhyay S, Redler B, Linstedt AD (2013). Shiga toxin-binding site for host cell receptor GPP130 reveals unexpected divergence in toxin-trafficking mechanisms. Mol Biol Cell 24, 2311–2318.
Olanow CW (2004). Manganese-induced parkinsonism and Parkinson's disease. Ann NY Acad Sci 1012, 209–223.
Petersen CM, Nielsen MS, Nykjaer A, Jacobsen L, Tommerup N, Rasmussen HH, Roigaard H, Gliemann J, Madsen P, Moestrup SK (1997). Molecular identification of a novel candidate sorting receptor purified from human brain by receptor-associated protein affinity chromatography. J Biol Chem 272, 3599–3605.
Potelle S, Dulary E, Climer L, Duvet S, Morelle W, Vicogne D, Lebredonchel E, Houdou M, Spriet C, Krzewinski-Recchi MA, *et al.* (2017). Manganese-induced turnover of TMEM165. Biochem J 474, 1481–1493.
Potelle S, Morelle W, Dulary E, Duvet S, Vicogne D, Spriet C, Krzewinski-Recchi MA, Morsomme P, Jaeken J, Matthijs G, *et al.* (2016). Glycosylation abnormalities in Gdt1p/TMEM165 deficient cells result from a defect in Golgi manganese homeostasis. Hum Mol Genet 25, 1489–1500.
Puri S, Bachert C, Fimmel CJ, Linstedt AD (2002). Cycling of early Golgi proteins via the cell surface and endosomes upon lumenal pH disruption. Traffic 3, 641–653.
Quistgaard EM, Madsen P, Groftehauge MK, Nissen P, Petersen CM, Thirup SS (2009). Ligands bind to Sortilin in the tunnel of a ten-bladed beta-propeller domain. Nat Struct Mol Biol 16, 96–98.
Rivera VM, Wang X, Wardwell S, Courage NL, Volchuk A, Keenan T, Holt DA, Gilman M, Orci L, Cerasoli F Jr, *et al.* (2000). Regulation of protein secretion through controlled aggregation in the endoplasmic reticulum. Science 287, 826–830.
Rizzo R, Parashuraman S, Mirabelli P, Puri C, Lucocq J, Luini A (2013). The dynamics of engineered resident proteins in the mammalian Golgi complex relies on cisternal maturation. J Cell Biol 201, 1027–1036.
Saito K, Katada T (2015). Mechanisms for exporting large-sized cargoes from the endoplasmic reticulum. Cell Mol Life Sci 72, 3709–3720.
Seddon AM, Curnow P, Booth PJ (2004). Membrane proteins, lipids and detergents: not just a soap opera. Biochim Biophys Acta 1666, 105–117.
Tartakoff AM (1983). Perturbation of vesicular traffic with the carboxylic ionophore monensin. Cell 32, 1026–1028.
Tewari R, Bachert C, Linstedt AD (2015). Induced oligomerization targets Golgi proteins for degradation in lysosomes. Mol Biol Cell 26, 4427–4437.
Tewari R, Jarvela T, Linstedt AD (2014). Manganese induces oligomerization to promote down-regulation of the intracellular trafficking receptor used by Shiga toxin. Mol Biol Cell 25, 3049–3058.
Willnow TE, Petersen CM, Nykjaer A (2008). VPS10P-domain receptors—regulators of neuronal viability and function. Nat Rev Neurosci 9, 899–909.
Wolins N, Bosshart H, Kuster H, Bonifacino JS (1997). Aggregation as a determinant of protein fate in post-Golgi compartments: role of the luminal domain of furin in lysosomal targeting. J Cell Biol 139, 1735–1745.